

Selected Paper

pH-Dependent Color-Change Behavior of Bis(*o*-phenylenediamine)-platinum(II) Complex and pH-Dependent Redox of Bis(*o*-semibenzoquinonediimine)platinum(II) Complex

Yosuke Konno and Nobuyuki Matsushita*

Department of Chemistry, Graduate School of Arts and Sciences, The University of Tokyo, 3-8-1 Komaba, Meguro-ku, Tokyo 153-8902

Received October 5, 2005; E-mail: cnmatsu@mail.ecc.u-tokyo.ac.jp

pH-Dependent color changes of an innocent diamineplatinum(II) complex, $[Pt(H_2L)_2]Cl_2$ ($[\mathbf{1}]Cl_2$), where H_2L is *o*-phenylenediamine, and the pH-dependent redox of non-innocent diimineplatinum(II) complexes, $[Pt(L)_2]$ (**2**) and $[\{Pt(L)_2\}_2]Cl_2$ ($[\mathbf{2}_2]Cl_2$), where L is *o*-semibenzoquinonediimine monoanion or neutral *o*-benzoquinonediimine, have been investigated by vis–NIR spectroscopy and cyclic voltammetry in solutions of various pH. The crystals of $[\mathbf{1}]Cl_2 \cdot 2H_2O$ and $[\mathbf{2}_2]Cl_2 \cdot 6H_2O$ have also been characterized by X-ray crystallography. $[\mathbf{1}]Cl_2$ in an aqueous solution changes from colorless either to purple or to yellow-green depending on the pH of the solution. The purple solution gave a neutral complex **2** and the yellow-green solution yielded $[\mathbf{2}_2]Cl_2 \cdot 6H_2O$. In the latter complex, the monocation, $[\mathbf{2}]^+$, dimerizes forming a weak Pt–Pt bond [3.0109(4) Å] with no bridging ligands. The spectroscopy of $[\mathbf{1}]Cl_2$ in the buffer solutions shows that the complex **2** is formed in the range of pH 4.6–5.8, while the complex $[\mathbf{2}]^+$ is generated in the range of pH 2.1–4.5. These results indicate that the one-electron redox process of $[\mathbf{2}]^+/\mathbf{2}$ depends on the pH of the solution. By adjusting the pH of the solution by adding acid or base, it is possible to reversibly control this redox process. This behavior is a kind of pH-dependent chromism because of their color being different.

Transition-metal complexes having non-innocent ligands such as dioxolenes,[1] dithiolenes,[2] and benzoquinonediimines[3,4] adopting three oxidation states (L^{2-}: catecholate-like dianions, L^-: π-radical semiquinonate monoanions, or L^0: neutral quinones) (Scheme 1), have been receiving much attention in view of the redox-activity of the ligand coupled with the central metal: e.g. valence tautomerization,[1c] partial oxidation producing molecular-based conductors,[2c] and so on. For the benzoquinonediimines, Balch and Holm[4] have reported that neutral, square-planar, diamagnetic complexes, $[M^{II}(L)_2]$ (M is Ni, Pd, or Pt, and L is *o*-semibenzoquinonediimine) are obtained by the reaction of *o*-phenylenediamine (H_2L) with metal salts in the presence of base and air. The existence of the complete five-membered series, $[M(L)_2]^z$ ($z = 2-, 1-, 0, 1+, 2+$), with four reversible one-electron-transfer processes has been established by polarography. Each electron-transfer process is ligand-based and the formal oxidation states of the central metal ions retain a divalent state. The one-electron oxidized species, $[M(L)_2]I$, obtained by the reaction of $[M(L)_2]$ with I_2 are paramagnetic ($S = 1/2$) with ligand-based character of the unpaired electron by ESR study. The doubly deprotonated form of *o*-phenylenediamine, $L^{2-,1-,0}$, functions as the non-innocent ligand, whereas the parent *o*-phenylenediamine, H_2L, acts as an innocent ligand.[3] We focus again on the metal complexes having the non-innocent *o*-semibenzoquinonediimine, because its undeprotonated, innocent *o*-phenylenediamine forms metal complexes.[3] So far, some *o*-phenylenediamine metal complexes have been synthesized and structurally characterized.[5] The existence of the metal complexes with the innocent parent ligand is different from cases of the dioxolene and dithiolene compounds. Sharma et al.[6] have recently reported the synthesis of the bis(*o*-phenylenediamine)platinum(II) complex, $[Pt(H_2L)_2]Cl_2$, isolated as a black powder. The black color is, however, inconsistent with the general observation that most tetraamineplatinum(II) complexes are colorless to pale-yellow. The color of the solid suggests the presence of impurities, although the authors have pointed nothing out. In our study, colorless plate-like single crystals of $[Pt(H_2L)_2]Cl_2 \cdot 2H_2O$ ($[\mathbf{1}]Cl_2 \cdot 2H_2O$) have been successfully obtained by careful recrystallization. The colorless crystals are soluble in water and its solution is colorless. Interestingly, the color of the aqueous solution changes gradually from colorless to either purple or yellow-green depending on the pH of the solution.

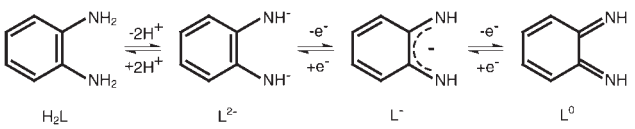

Scheme 1.

In this paper, we demonstrate that the pH-dependent color-change behavior is ascribed to the deprotonation and oxidation of $[\mathbf{1}]Cl_2$: that is, the formation of either $[Pt(L)_2]$ (**2**) or its one-electron-oxidized species, $[Pt(L)_2]^+$ ($\mathbf{2}^+$), depending on the pH of the solution, where L denotes the *o*-semibenzoquinonediimine monoanion or neutral *o*-benzoquinonediimine. We also show that the one-electron redox process of $[\mathbf{2}]^+/\mathbf{2}$ depends on the pH of the solution. In the crystal, the monocations $[\mathbf{2}]^+$ form an unsupported dimer, $[\{Pt(L)_2\}_2]Cl_2 \cdot 6H_2O$ ($[\mathbf{2}_2]Cl_2 \cdot 6H_2O$), with a weak Pt–Pt bond. The X-ray crystallography of $[\mathbf{1}]Cl_2 \cdot 2H_2O$ and $[\mathbf{2}_2]Cl_2 \cdot 6H_2O$ are also reported.

Published on the web July 4, 2006; doi:10.1246/bcsj.79.1046

Experimental

Materials. $H_2[PtCl_6]\cdot 6H_2O$ was purchased form Furuya Metal Co., Ltd. *o*-Phenylenediamine was purchased from Kanto Chemical Co., Inc. All reagents were used without further purification. $PtCl_2$ was prepared according to the literature method.[7]

$[Pt(H_2L)_2]Cl_2\cdot 2H_2O$ ($[1]Cl_2\cdot 2H_2O$). The complex $[1]Cl_2$ was prepared by the procedure of Sharma et al.[6] To a methanol solution of $PtCl_2$ (1.0 mmol/10 mL of CH_3OH) was added *o*-phenylenediamine (2.0 mmol). The solution was stirred at 55 °C for 12 h. A white-to-gray powder solid was obtained. The color of the powder depended on batches. Recrystallization by adding hydrochloric acid to an aqueous solution of the white-to-gray powder solid gave colorless plate-like crystals suitable for single-crystal X-ray analysis. Yield 23%. Anal. Found: C, 27.55; H, 3.89; N, 10.57%. Calcd for $C_{12}H_{20}Cl_2N_4O_2Pt$: C, 27.81; H, 3.89; N, 10.81%. Loss of weight in thermogravimetry: Found: 7.00%. Calcd for $C_{12}H_{20}Cl_2N_4O_2Pt$: $2H_2O$, 6.95%.

$[Pt(L)_2]$ (2). An aqueous solution of $[1]Cl_2\cdot 2H_2O$ (1.0 mmol/100 mL of H_2O) was adjusted to pH 10 by adding 25% aqueous ammonia. This solution was stirred for 12 h in air. A purple powder precipitated and was collected by filtration, then washed with 10 mL of water and acetone. Yield 99%. Vis–NIR absorption (ν_{max}/cm^{-1} ($\varepsilon/dm^3\,mol^{-1}\,cm^{-1}$), dimethyl sulfoxide): 14000 (102700).

$[\{Pt(L)_2\}_2]Cl_2\cdot 6H_2O$ ($[2_2]Cl_2\cdot 6H_2O$). To an aqueous solution of $[1]Cl_2\cdot 2H_2O$ (0.1 mmol/30 mL of H_2O) was added a few drops of 1.0 M hydrochloric acid (M = mol dm^{-3}). The solution was sealed in a screw-cap vial. Standing of the solution at room temperature for 3 weeks afforded dark blue needle crystals suitable for single-crystal X-ray analysis. Yield 10%. Vis–NIR absorption (ν_{max}/cm^{-1} ($\varepsilon/dm^3\,mol^{-1}\,cm^{-1}$), water): 12300 (38200), 22800 (25500). Anal. Found: C, 29.12; H, 3.60; N, 11.18%. Calcd for $C_{24}H_{36}Cl_2N_8O_6Pt_2$: C, 29.01; H, 3.65; N, 11.28%. Loss of weight in thermogravimetry: Found: 10.47%. Calcd for $C_{24}H_{36}Cl_2N_8O_6Pt_2$: $6H_2O$, 10.88%.

Elemental analysis was carried out by the Laboratory of Organic Elemental Analysis, Department of Chemistry, Graduate School of Science, The University of Tokyo.

X-ray Crystallography. Each single crystal of $[1]Cl_2\cdot 2H_2O$ and $[2_2]Cl_2\cdot 6H_2O$ was mounted on a glass fiber. Intensity data were measured with a Rigaku R-AXIS RAPID Imaging Plate diffractometer at 23 °C for $[1]Cl_2\cdot 2H_2O$ and at −120 °C for $[2_2]Cl_2\cdot 6H_2O$. The diffractometer was equipped with graphite-monochromated Mo Kα radiation (0.7107 Å) and with a Rigaku low-temperature device. Intensity data were corrected for Lorentz-polarization effects and absorption factors based on a multi-scan method. The structures of $[1]Cl_2\cdot 2H_2O$ and $[2_2]Cl_2\cdot 6H_2O$ were solved by the direct method and conventional heavy-atom method, respectively. The refinements were performed on F^2 by full-matrix least-squares methods with anisotropic displacement parameters for non-H atoms. All H atoms of both compounds were located from the difference Fourier map. All H atoms of $[1]Cl_2\cdot 2H_2O$ were isotropically refined. In $[2_2]Cl_2\cdot 6H_2O$, the H atoms of the complex were isotropically refined and those of water molecules were not refined.

Programs used were *SHELXS*97[8] for solutions, *SHELXL*97[8] for refinements, *ABSCOR*[9] for absorption corrections and *ORTEP*-3[10] for drawing structures. Details of crystal data and refinement for $[1]Cl_2\cdot 2H_2O$ and $[2_2]Cl_2\cdot 6H_2O$ are listed in Table 1.

Crystallographic data have been deposited with Cambridge Crystallographic Data Centre: Deposition numbers CCDC-298847 for compound $[1]Cl_2\cdot 2H_2O$ and CCDC-298848 for compound $[2_2]Cl_2\cdot 6H_2O$. Copies of the data can be obtained free of charge via http://www.ccdc.cam.ac.uk/conts/retrieving.html (or form the Cambridge Crystallographic Data Centre, 12, Union Road, Cambridge, CB2 1EZ, UK; Fax: +44 1223 336033; e-mail: deposit@ccdc.cam.ac.uk).

Physical Measurements. Thermogravimetry (TG) was examined on a TA Instruments TGA2950 at a scanning rate of 10 °C min^{-1} from 25 to 200 °C. Powder X-ray diffraction (XRD) measurements were performed at room temperature using a Rigaku Multi Flex X-ray diffractometer equipped with graphite-monochromated Cu Kα radiation (1.5418 Å) with θ–2θ scans. Vis–NIR absorption spectra were recorded on a JASCO V-530 spectrophotometer. The buffer solutions were HCl/KCl for pH 2.1 and CH_3COOH/CH_3COONa for pH 3.5–5.8. Single-crystal polarized absorption and reflection spectra were measured with a microspectroscopic system, composed of an OLYMPUS BX60 microscope, a polarizing plate, a tungsten lamp, and an Ocean Optics USB2000 fiber-optic multi-channel CCD spectrometer. Cyclic voltammograms were recorded at 25 °C in dimethyl sulfoxide (DMSO) solutions containing 0.1 M $[(n\text{-}C_4H_9)_4N]ClO_4$ as a supporting electrolyte under a N_2 atmosphere on a Hokuto Denko HSV-100 automatic polarization system. A Pt working electrode, a Pt wire auxiliary electrode, and a Ag/Ag^+ reference electrode, purchased from BAS, were used. The half-wave potential of Fc/Fc^+ (Fc = ferrocene) was +0.06 V against the reference electrode. The pH dependence of the redox and rest potential was measured by adjusting the pH of the solution with 0.1 and 0.01 M hydrochloric acid or aqueous NaOH solutions. Spectroelectrochemistry was performed using the Hokuto Denko HSV-100 automatic polarization system and the Ocean Optics USB2000 fiber-optic multi-channel CCD spectrometer. A Pt grid working electrode, a Pt auxiliary-reference electrode, and a spectroelectrochemical cell, purchased from BAS, were used. The pH of the solution was measured with a TOA Model HM-21P pH meter standardized with buffers of pH 4.01 and 6.86.

Results and Discussion

Preparation and Crystallization of $[Pt(H_2L)_2]Cl_2$. The complex $[Pt(H_2L)_2]Cl_2$ ($[1]Cl_2$) was prepared from $PtCl_2$ and *o*-phenylenediamine (H_2L) according to the procedure of Sharma et al.[6] A white-to-gray powder solid was obtained in our study, although the authors reported that the complex, $[1]Cl_2$, was black. The color of the solid suggests the presence of impurities because most tetraammineplatinum(II) complexes are, in general, colorless to pale yellow. Recrystallization was performed to purify the crude powder solid and to obtain single crystals suitable for X-ray crystallography.

In the recrystallization, addition of hydrochloric acid to an aqueous solution of $[1]Cl_2$ prevented the deprotonation of the ligand and immediately precipitated the crystals. Colorless plate-like crystals suitable for the X-ray crystallography were obtained. The elemental analysis, thermogravimetry, and X-ray analysis show that the colorless crystals are a dihydrate of $[1]Cl_2$, formulated as $[Pt(H_2L)_2]Cl_2\cdot 2H_2O$ ($[1]Cl_2\cdot 2H_2O$). A single-crystal polarized absorption spectrum measured on the (100) crystal face showed no spectral features in the visible region. This result is consistent with the fact that tetraammineplatinum(II) complexes have, in general, no absorption bands in the visible region.

pH-Dependent Color Change. Dissolution of the crystal

Table 1. Crystallographic Data for $[Pt(H_2L)_2]Cl_2 \cdot 2H_2O$ ($[\mathbf{1}]Cl_2 \cdot 2H_2O$) and $[\{Pt(L)_2\}_2]Cl_2 \cdot 6H_2O$ ($[\mathbf{2}_2]Cl_2 \cdot 6H_2O$)

	$[\mathbf{1}]Cl_2 \cdot 2H_2O$	$[\mathbf{2}_2]Cl_2 \cdot 6H_2O$
Formula	$C_{12}H_{20}Cl_2N_4O_2Pt$	$C_{24}H_{36}Cl_2N_8O_6Pt_2$
Formula weight	518.31	993.69
Crystal system	orthorhombic	triclinic
Space group	*Pbam* (No. 55)	$P\bar{1}$ (No. 2)
a/Å	8.6534(9)	11.6156(13)
b/Å	12.9027(10)	11.6772(12)
c/Å	7.4328(4)	6.7659(7)
α/°	90	93.558(4)
β/°	90	101.679(5)
γ/°	90	118.616(5)
V/Å^3	829.89(12)	775.32(14)
Z	2	1
Temperature/K	296	153
D_{calcd}/g cm^{-3}	2.074	2.128
μ/mm^{-1}	8.784	9.236
θ range/°	3.2–32.6	3.1–32.5
Crystal color	colorless, plate	dark blue, needle
Crystal size/mm^3	0.385 × 0.360 × 0.016	0.175 × 0.100 × 0.038
No. of measured reflns	21618	10624
No. of independent reflns	1602 [$R_{int} = 0.033$]	5275 [$R_{int} = 0.019$]
No. of observed reflns	1309 [$F_o^2 > 2\sigma(F_o^2)$]	4871 [$F_o^2 > 2\sigma(F_o^2)$]
No. of parameters	76	245
R[a)]	0.0208	0.0188
wR[a)]	0.0643	0.0488
S[a)]	1.126	1.461
Weighting Scheme	$w = 1/[\sigma^2(F_o^2) + (0.0450P)^2]$, where $P = (F_o^2 + 2F_c^2)/3$	$w = 1/[\sigma^2(F_o^2) + (0.0212P)^2]$, where $P = (F_o^2 + 2F_c^2)/3$

a) $R = (\Sigma||F_o| - |F_c||)/\Sigma|F_o|$ for observed reflections, $wR = [\{\Sigma(w(F_o^2 - F_c^2)^2)\}/\Sigma(w(F_o^2)^2)]^{1/2}$ for independent reflections. $S = [\{\Sigma(w(F_o^2 - F_c^2)^2)\}/(n - p)]^{1/2}$ where n and p are the No. of the reflection and the parameters in the refinement, respectively.

$[\mathbf{1}]Cl_2 \cdot 2H_2O$ in water gave a colorless solution, which changed gradually to yellow-green on standing at room temperature. Figure 1 shows a time-course change of vis–NIR absorption spectra after dissolution of $[\mathbf{1}]Cl_2 \cdot 2H_2O$ in water. Two characteristic absorption bands appear at 12300 and 22800 cm^{-1}. The color change resulting from the appearance of the absorption bands is remarkably suppressed by adding hydrochloric acid to the colorless solution. In contrast, the colorless solution changes rapidly to purple by adding an aqueous NaOH solution, and after a while, a purple powder solid precipitates. A time-course change of vis–NIR absorption spectra after the addition of the aqueous NaOH solution to the colorless solution before producing the precipitate is shown in Fig. 2. A broad absorption band appears over the range 15000–20000 cm^{-1}.

These results suggest that the color-change behavior of the aqueous solution of $[\mathbf{1}]Cl_2 \cdot 2H_2O$ depends on the pH of the solution. Examinations of the dissolution of $[\mathbf{1}]Cl_2 \cdot 2H_2O$ in buffer solutions of various pH values between 2.1 and 5.8 gave two types of absorption spectra. One is a case of absorption spectra in the buffer solutions of pH 2.1–4.5, and the other is in the buffer solutions of pH 4.6–5.8. The former is in agreement with that of the yellow-green solution as shown in Fig. 1. The latter is consistent with that of the purple solution as shown in Fig. 2. These results indicate that the color-change behavior of the aqueous solution of $[\mathbf{1}]Cl_2 \cdot 2H_2O$ is pH-

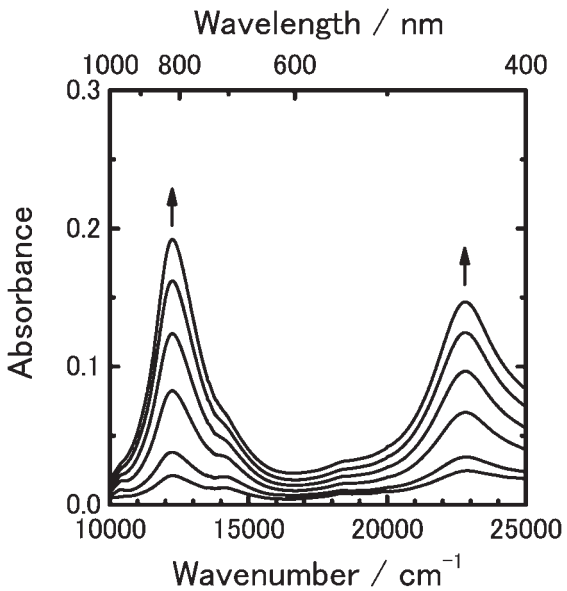

Fig. 1. Time-course change of absorption spectra after dissolution of $[\mathbf{1}]Cl_2 \cdot 2H_2O$ in water (concentration: 3.859 × 10^{-3} M) at 30 °C, recorded every 20 min.

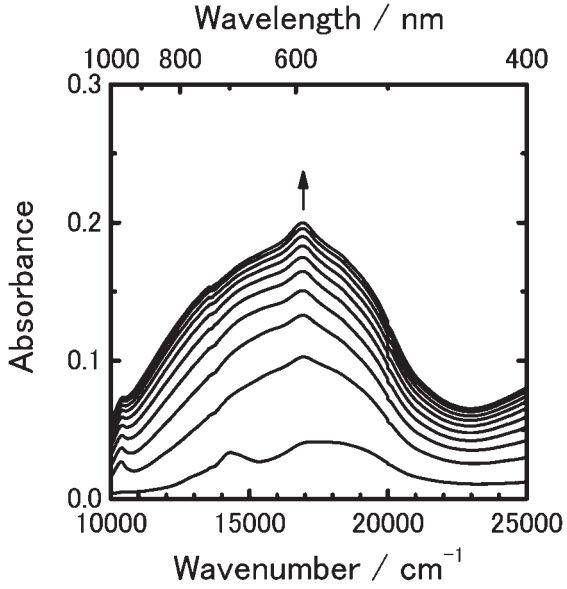

Fig. 2. Time-course change of absorption spectra after addition of 0.01 M NaOH to colorless aqueous solution of [**1**]$Cl_2 \cdot 2H_2O$ (concentration: 7.718×10^{-4} M) at 30 °C, recorded every 10 min.

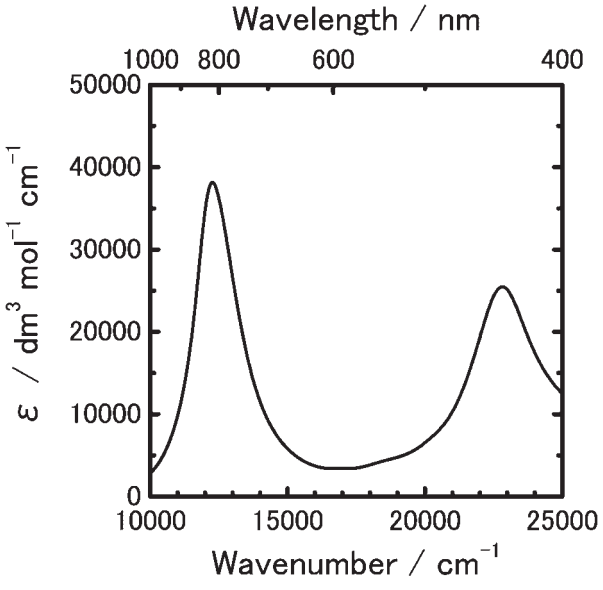

Fig. 3. Absorption spectrum of [$\mathbf{2}_2$]$Cl_2 \cdot 6H_2O$ in water (concentration: 4.831×10^{-5} M) at 25 °C.

dependent and has a threshold between pH 4.5 and 4.6.

Although the addition of hydrochloric acid to the colorless solution, which gave a solution of pH less than 2, suppressed the color change, addition to the color-changed solutions could not reproduce the colorless solution. The color-change behavior between the colorless solution and the colored solutions was irreversible.

Products in Color Change. Standing the yellow-green solution turned from the colorless solution of [**1**]$Cl_2 \cdot 2H_2O$ in the acidic conditions for one week, gave dark blue needle-like crystals. On the other hand, in the neutral to basic condition, the purple powder solid precipitated from the purple solution, which initially was a colorless solution. Their products have been characterized in order to clarify the origin of the color-change behavior.

A powder XRD pattern of the purple powder solid from the solution of [**1**]$Cl_2 \cdot 2H_2O$ is in good agreement with that of compound **2** prepared by the literature method.[4] An intense absorption band of the purple powder solid in a DMSO solution (14000 cm^{-1}, $\varepsilon = 102700$ dm^3 mol^{-1} cm^{-1}) also agrees with that of **2** in a DMSO solution (14100 cm^{-1}, $\varepsilon = 96700$ dm^3 mol^{-1} cm^{-1}) reported in the literature.[4] These results indicate that the purple powder solid produced from the solution of [**1**]$Cl_2 \cdot 2H_2O$ in the neutral to basic condition is the neutral complex, [Pt(L)$_2$] (**2**). The absorption spectrum of **2** in a DMSO solution is different from that of the purple aqueous solution derived from [**1**]$Cl_2 \cdot 2H_2O$ in the neutral to basic condition as shown in Fig. 2. The spectrum of the purple aqueous solution is, however, consistent with that of **2** in a basic aqueous solution, which was barely observed since it is difficult to obtain a sufficient concentration of the solution because of the very low solubility of **2** in water (Fig. S1a). The addition of water to the DMSO solution changed its absorption spectrum to that of the aqueous solution (Fig. S1b). In addition, the spectrum of the aqueous solution is similar to that of the single crystal (Fig. S1c). These dependences of the absorption spectrum suggest that the electronic state of **2** in solution phases strongly depends on an aggregation of the molecules of **2** based on solvation. It is concluded that the color-change behavior from colorless to purple is due to the formation of **2**, of which the ligand is in the non-innocent state, from [**1**]Cl_2, of which the ligand is in the innocent state, and that the change originates from the deprotonation and the oxidation.

As for the dark blue needle-like crystals obtained from the yellow-green solution, single-crystal X-ray analysis reveals that the crystals are formulated as [{Pt(L)$_2$}$_2$]$Cl_2 \cdot 6H_2O$ ([$\mathbf{2}_2$]$Cl_2 \cdot 6H_2O$). In this complex, [$\mathbf{2}_2$]Cl_2, the monocation complex, [Pt(L)$_2$]$^+$ ([**2**]$^+$), dimerizes with a weak Pt–Pt bond of 3.0109(4) Å. Details of the X-ray crystallography of [$\mathbf{2}_2$]$Cl_2 \cdot 6H_2O$ are described below. Figure 3 shows the absorption spectrum of [$\mathbf{2}_2$]$Cl_2 \cdot 6H_2O$ dissolved in water. It agrees completely with that of the yellow-green solution as shown in Fig. 1. The spectrum displays two characteristic absorption bands (12300 cm^{-1}, $\varepsilon = 38200$ dm^3 mol^{-1} cm^{-1} and 22800 cm^{-1}, $\varepsilon = 25500$ dm^3 mol^{-1} cm^{-1}). The spectrum is independent of concentration from 1×10^{-6} to 2×10^{-4} mol dm^{-3}. Wieghardt et al.[11] have reported that solutions of one-electron-oxidized species of analogous nickel(II) complexes with *o*-semibenzoquinonediimine derivatives are ESR silent showing dimerization of these radical cations, and that a solution of the one-electron-oxidized species of analogous platinum(II) complexes with the *o*-semibenzoquinonediimine derivative exhibits an ESR spectrum in spite of the fact that the platinum(II) complex dimerizes in the solid state. In addition, the crystalline solid of [$\mathbf{2}_2$]$Cl_2 \cdot 6H_2O$ displays an ESR spectrum in our preliminary measurement. From these facts, the dimer structure of [**2**]$^+$ in the crystalline phase is presumed to be at least incompletely kept in the solution phase. This presumption is also supported by the single-crystal reflectance spectrum (Fig. 4) being similar to the solution absorption spectrum (Fig. 3).

The solution absorption spectrum of [$\mathbf{2}_2$]$Cl_2 \cdot 6H_2O$ is in good agreement with that of a species oxidized electrochemi-

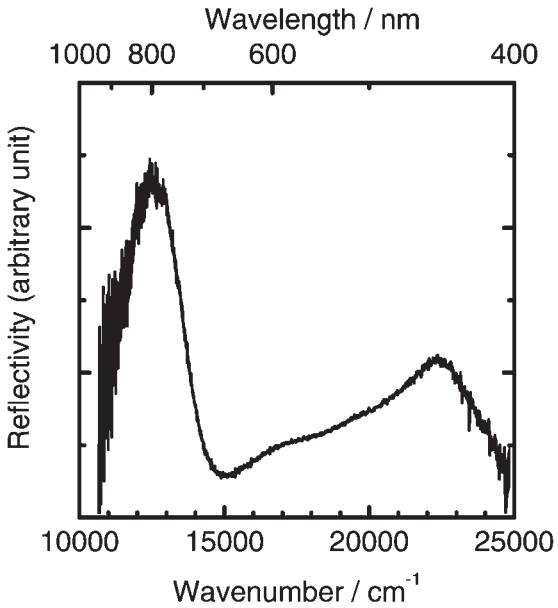

Fig. 4. Single-crystal reflectance spectrum of $[\mathbf{2}_2]Cl_2 \cdot 6H_2O$ at room temperature.

cally from **2** in the DMSO solution, which has two absorption bands at 12100 and 22400 cm^{-1} (Fig. 5a). The reverse reduction process from the one-electron-oxidized species to **2** is also observed as shown in Fig. 5b. These results indicate that the complex, $[\mathbf{2}_2]Cl_2$ obtained from $[\mathbf{1}]Cl_2$, is identical to the one-electron-oxidized species of **2**. Thus, the color-change behavior from colorless to yellow-green is attributed to the formation of the one-electron-oxidized species $[\mathbf{2}]^+$.

pH-Dependent Redox. As above described, the color of $[\mathbf{1}]Cl_2 \cdot 2H_2O$ changes to purple in buffer solutions of pH 4.6–5.8 and to yellow-green in buffer solutions of pH 2.1–4.5. The characterization of their products indicates that the neutral complex **2** is formed in the range of pH 4.6–5.8, whereas the one-electron-oxidized species $[\mathbf{2}]^+$ is generated in the range of pH 2.1–4.5. In the latter case, $[\mathbf{2}]^+$ is generated probably by way of **2** as an intermediate. Consideration of the formation of **2** in both cases suggests that the one-electron redox process of $[\mathbf{2}]^+/\mathbf{2}$ (Scheme 2) depends on the pH of the solution. Adding H_2SO_4 as an acid to the DMSO solution of **2** causes the formation of the one-electron-oxidized species, as shown in Fig. 6a. This spectral change is similar to that of the electrochemical oxidation (Fig. 5a). Then, the absorption spectrum reverts to that of **2** by adding triethylamine as a base to the resultant DMSO solution containing the one-electron-oxidized species, as shown in Fig. 6b.

From the results of the spectral changes, we could expect that the potential of the one-electron redox process of $[\mathbf{2}]^+/\mathbf{2}$ depended on the pH of the solution. The redox process of **2** has been already established as four reversible ligand-centered processes caused by one-electron transfers by polarography.[4] The relationship between the redox potentials and pH, however, had not been studied. Therefore, we have measured cyclic voltammograms of **2** at various pH values.

As shown in Fig. 7, the cyclic voltammogram of **2** in a DMSO solution, of which the pH was 5.6, displayed four reversible redox waves at −2.13, −1.44, −0.26, and +0.28 V

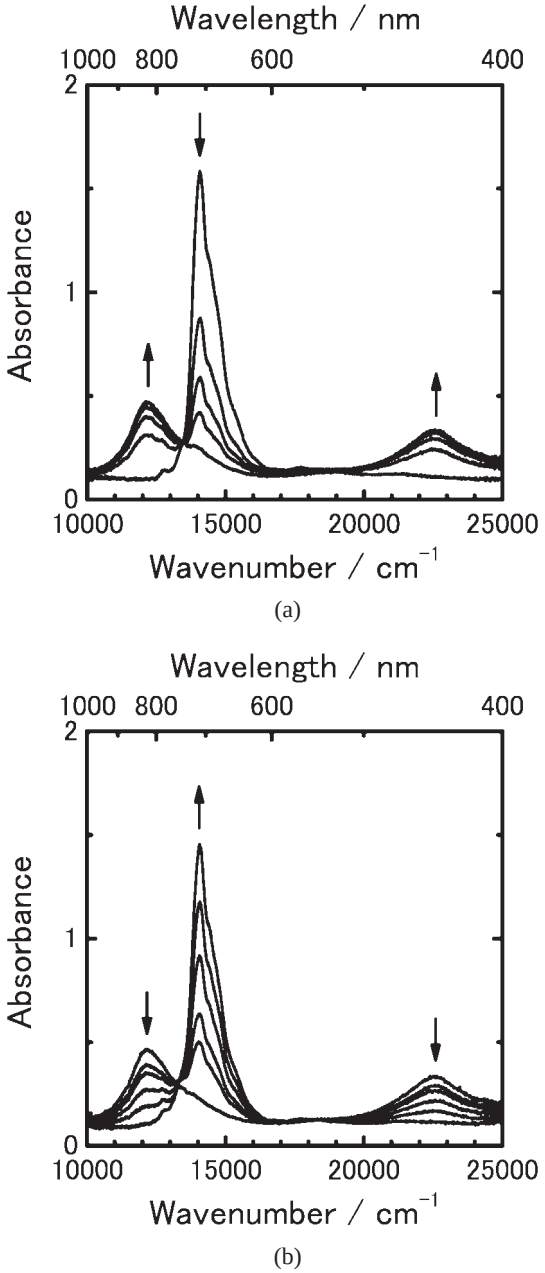

Fig. 5. Spectral changes accompanying the electrochemical oxidation of **2** at +0.4 V (a) and the reduction of its one-electron-oxidized species at −0.2 V (b) in DMSO (0.1 M $[(n\text{-}C_4H_9)_4N]ClO_4$).

$$[Pt(L)_2] \quad (\mathbf{2}) \quad \underset{+e^-}{\overset{-e^-}{\rightleftharpoons}} \quad [Pt(L)_2]^+ \quad ([\mathbf{2}]^+)$$

Scheme 2.

(vs Ag/Ag^+). These values are in agreement with those of the polarography.[4] The first oxidation wave ($E^{ox}_{1/2} = -0.26$ V) is insensitive to air and water, whereas the other redox waves are sensitive to air and trace amounts of water. The pH dependence of the potential of the first oxidation wave ($E^{ox}_{1/2}$) is plotted in Fig. 8. Contrary to our assumption, the values of $E^{ox}_{1/2}$ are invariable in the narrow range of −0.26 to −0.28 V over the range of pH 4.0–8.0. In contrast, the rest

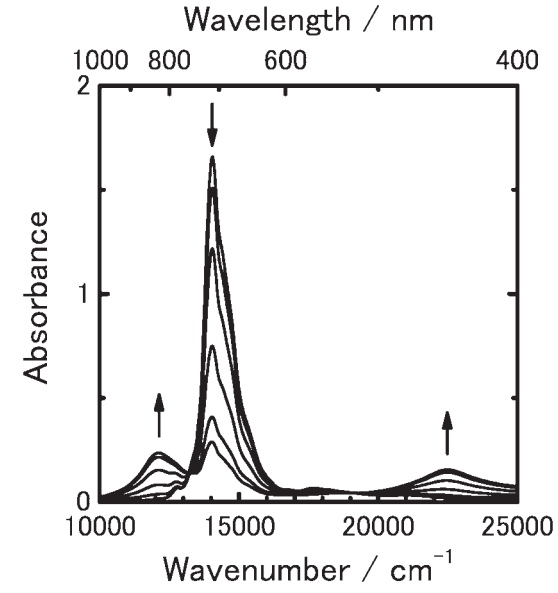

(a)

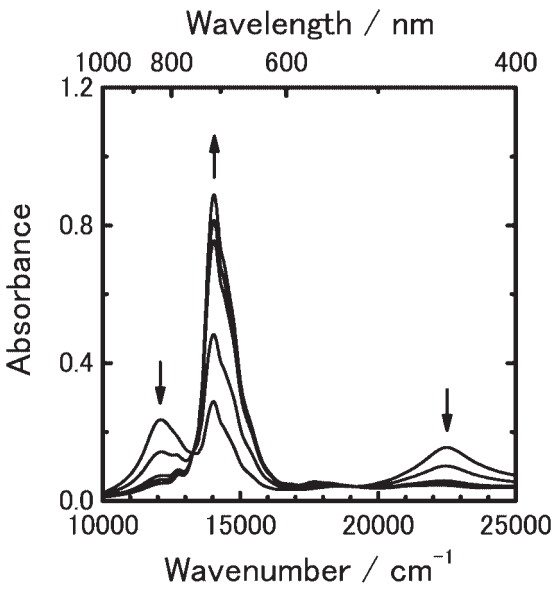

(b)

Fig. 6. Spectral changes caused by adding H_2SO_4 (1.0 M, in DMSO) to **2** in DMSO (concentration: 1.964×10^{-5} M) at 25 °C (a) and by adding triethylamine (1.0 M, in DMSO) to the resultant DMSO solution (b).

potential of the solution increases from −0.45 to −0.23 V with decreasing pH over this range (Fig. 8). The rest potential crosses over $E^{ox}_{1/2}$ around pH 5.0 and exceeds it in the pH values between 4.0 and 5.0. It is interesting that the rest potential shifts toward the positive side across $E^{ox}_{1/2}$ by adjusting the pH of the solution from 5.6 to 4.0. As a result, the redox process of $[\mathbf{2}]^+/\mathbf{2}$ is reversibly controlled by the pH of the solution, although the redox potential of $[\mathbf{2}]^+/\mathbf{2}$ is pH-independent. This behavior is a kind of pH-dependent chromism because of their colors being remarkably different.

Crystal Structures. The molecular structures of $[\mathbf{1}]Cl_2 \cdot 2H_2O$ and $[\mathbf{2}_2]Cl_2 \cdot 6H_2O$ are shown in Figs. 9 and 10, respec-

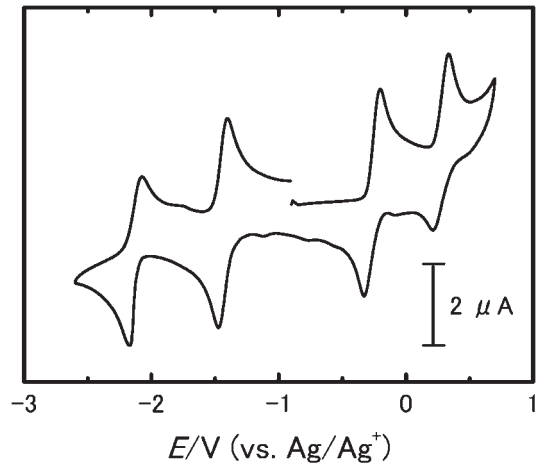

Fig. 7. Cyclic voltammogram of **2** in DMSO containing $[(n\text{-}C_4H_9)_4N]ClO_4$ (0.1 M) as a supporting electrolyte at a Pt working electrode, a Ag/Ag^+ reference electrode, and scanning rate 400 mV s^{-1}.

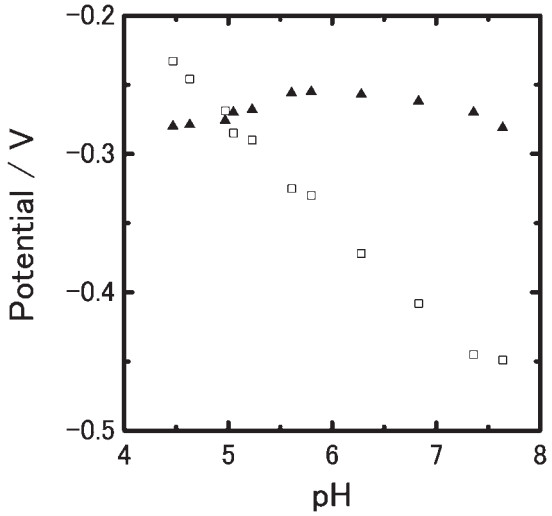

Fig. 8. pH Dependence of the redox potential for the first oxidation wave and the rest potential of **2** in DMSO (0.1 M $[(n\text{-}C_4H_9)_4N]ClO_4$). Solid triangles and open squares indicate the redox potential and the rest potential, respectively.

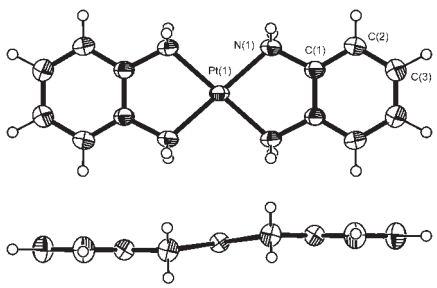

Fig. 9. Perspective views of the platinum complex cation in crystals of $[\mathbf{1}]Cl_2 \cdot 2H_2O$ with the atomic numbering scheme; a top view (on top) and a side view (on bottom). Displacement ellipsoids are drawn at the 50% probability level for non-H atoms.

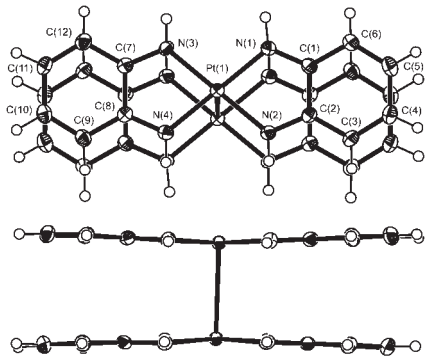

Fig. 10. Perspective views of the unsupported platinum(II) complex dimer in crystals of $[\mathbf{2}_2]Cl_2 \cdot 6H_2O$ with the atomic numbering scheme; a top view (on top) and a side view (on bottom). Displacement ellipsoids are drawn at the 50% probability level for non-H atoms.

Table 2. Selected Bond Distances (Å) and Angles (°) for $[\mathbf{1}]Cl_2 \cdot 2H_2O$ and $[\mathbf{2}_2]Cl_2 \cdot 6H_2O$

		$[\mathbf{1}]Cl_2 \cdot 2H_2O$	
Pt(1)–N(1)	2.0402(17)	C(1)–C(2)	1.379(3)
N(1)–C(1)	1.450(2)	C(2)–C(3)	1.389(4)
C(1)–C(1)[a]	1.384(3)	C(3)–C(3)[a]	1.365(6)
N(1)–Pt(1)–N(1)[a]	83.23(9)	N(1)–C(1)–C(2)	122.48(15)
N(1)–Pt(1)–N(1)[b]	96.79(9)	C(2)–C(1)–C(1)[a]	120.33(11)
Pt(1)–N(1)–C(1)	110.68(10)	C(1)–C(2)–C(3)	119.1(2)
N(1)–C(1)–C(1)[a]	117.19(9)	C(2)–C(3)–C(3)[a]	120.53(15)
		$[\mathbf{2}_2]Cl_2 \cdot 6H_2O$	
Pt(1)–Pt(1)[c]	3.0109(4)	C(2)–C(3)	1.423(4)
Pt(1)–Pt(1)[d]	4.2063(4)	C(3)–C(4)	1.364(4)
Pt(1)–N(1)	1.980(2)	C(4)–C(5)	1.431(5)
Pt(1)–N(2)	1.978(2)	C(5)–C(6)	1.364(4)
Pt(1)–N(3)	1.972(2)	C(1)–C(6)	1.427(4)
Pt(1)–N(4)	1.980(2)	C(7)–C(8)	1.455(4)
N(1)–C(1)	1.320(3)	C(8)–C(9)	1.425(4)
N(2)–C(2)	1.326(3)	C(9)–C(10)	1.359(4)
N(3)–C(7)	1.322(3)	C(10)–C(11)	1.435(4)
N(4)–C(8)	1.323(3)	C(11)–C(12)	1.355(4)
C(1)–C(2)	1.461(4)	C(7)–C(12)	1.427(4)
N(1)–Pt(1)–N(2)	78.99(9)	C(2)–C(1)–C(6)	119.5(2)
N(1)–Pt(1)–N(3)	100.61(9)	C(1)–C(2)–C(3)	119.4(2)
N(2)–Pt(1)–N(4)	100.91(9)	C(2)–C(3)–C(4)	118.9(3)
N(3)–Pt(1)–N(4)	78.98(9)	C(3)–C(4)–C(5)	121.8(3)
Pt(1)–N(1)–C(1)	117.01(18)	C(4)–C(5)–C(6)	121.4(3)
Pt(1)–N(2)–C(2)	116.78(18)	C(1)–C(6)–C(5)	118.9(3)
Pt(1)–N(3)–C(7)	117.25(18)	C(8)–C(7)–C(12)	119.3(2)
Pt(1)–N(4)–C(8)	116.60(18)	C(7)–C(8)–C(9)	119.7(2)
N(1)–C(1)–C(2)	113.5(2)	C(8)–C(9)–C(10)	118.8(3)
N(2)–C(2)–C(1)	113.5(2)	C(9)–C(10)–C(11)	121.4(3)
N(3)–C(7)–C(8)	113.3(2)	C(10)–C(11)–C(12)	121.9(3)
N(4)–C(8)–C(7)	113.9(2)	C(7)–C(12)–C(11)	118.8(3)

a) Symmetry operation: $x, y, -z$. b) Symmetry operation: $-x, -y, z$. c) Symmetry operation: $1-x, 1-y, 1-z$. d) Symmetry operation: $1-x, 1-y, -z$.

Table 3. Hydrogen-Bonding Geometries (Å, °) for $[\mathbf{1}]Cl_2 \cdot 2H_2O$ and $[\mathbf{2}_2]Cl_2 \cdot 6H_2O$

D–H···*A*	*D*–H	H···*A*	*D*···*A*	*D*–H···*A*
		$[\mathbf{1}]Cl_2 \cdot 2H_2O$		
N(1)–H(1A)···Cl(1)[a]	0.91(4)	2.42(5)	3.2385(17)	150(4)
N(1)–H(1B)···O(1)	0.86(3)	2.09(2)	2.913(2)	160(2)
O(1)–H(4)···Cl(1)[b]	0.86(5)	2.20(5)	3.055(3)	176(11)
O(1)–H(5)···Cl(1)	0.86(4)	2.24(4)	3.097(3)	176(3)
		$[\mathbf{2}_2]Cl_2 \cdot 6H_2O$		
N(1)–H(1)···Cl(1)	0.88(5)	2.47(5)	3.342(2)	172(5)
N(2)–H(2)···O(1)	0.84(4)	2.13(4)	2.962(3)	173(3)
N(3)–H(7)···O(2)	0.87(4)	2.08(4)	2.932(3)	167(4)
N(4)–H(8)···O(3)	0.83(5)	2.07(5)	2.895(4)	172(5)
O(1)–H(13)···O(2)[c]	0.76	2.01	2.765(3)	167
O(1)–H(14)···Cl(1)[d]	0.82	2.36	3.161(3)	166
O(2)–H(15)···Cl(1)	0.87	2.31	3.140(3)	161
O(2)–H(16)···Cl(1)[e]	0.84	2.33	3.164(2)	171
O(3)–H(17)···Cl(1)[c]	0.87	2.39	3.239(3)	167
O(3)–H(18)···O(1)	0.74	2.30	3.004(5)	159

a) Symmetry operation: $1/2-x, -1/2+y, z$. b) Symmetry operation: $-1/2+x, 1/2-y, 1-z$. c) Symmetry operation: $1-x, 1-y, 1-z$. d) Symmetry operation: $1+x, y, z$. e) Symmetry operation: $-x, 1-y, -z$.

tively. Selected bond distances and angles are listed in Table 2 and hydrogen-bonding geometries are summarized in Table 3.

In $[\mathbf{1}]Cl_2 \cdot 2H_2O$, the Pt atom is coordinated by four N atoms of two ligands. The PtN_4 plane and each $C_6H_4N_2$ ligand plane are not coplanar with a dihedral angle of 8.9(1)°. The Pt–N distance [2.040(2) Å] is in agreement with those of other bis(diamine)platinum(II) chelate complexes [2.039(3) and 2.046(3) Å for $[Pt(en)_2]Cl_2$[12] (en = ethylenediamine) and 2.050(6)–2.062(6) Å for $[Pt(pn)_2]Cl_2$[13] (pn = propylenediamine)]. The N–C distance [1.450(2) Å] is consistent with the single N–C bond distance. The C–C distances [1.365(6)–1.389(4) Å; average 1.379 Å] agree well with those of a benzene ring. These results of the bond distance show that the ligand coordinates to the Pt atom as aromatic *o*-phenylenediamine in the crystal of $[\mathbf{1}]Cl_2 \cdot 2H_2O$. In addition, the H atoms located from the difference Fourier map indicate that the N atoms coordinating to the Pt atom are the amino group. The existence of hydrogen bonds between the N atom and the Cl^- ion [N···Cl = 3.239(2) Å] and between the N atom and the O atom of a water molecule of crystallization [N···O = 2.913(2) Å] also demonstrates that the ligand coordinates to the Pt atom as the aromatic diamine.

The crystal of $[\mathbf{2}_2]Cl_2 \cdot 6H_2O$ comprises an unsupported platinum(II) complex dimer, $[\{Pt(L)_2\}_2]^{2+}$, with a short contact of Pt–Pt [3.0109(4) Å], Cl^- ions, and water of crystallization. Figure 10 shows the structure of the unsupported platinum(II) complex dimer dication, $[\{Pt(L)_2\}_2]^{2+}$. Since the midpoint between the two Pt atoms in the dimer is located at an inversion center, two monomer units of the dimer are crystallographically equivalent and adopt an eclipsed configuration. Neither monomer unit is planar and each Pt atom slightly deviates from the N_4 plane to the center of the dimer by 0.093(1) Å, as shown in Fig. 10. These suggest a bonding interaction

between the Pt atoms. The bond distances of two crystallographically independent ligands in the monomer unit are in agreement with each other. Similar unsupported platinum(II) complex dimer structures have been reported for $[\{Pt(L)_2\}_2](CF_3SO_3)_2$,[14] $[cis\text{-}\{Pt(^{N\text{-}Ph}L)_2\}_2](CF_3SO_3)_2\cdot 2C_6H_6$,[15] and $[trans\text{-}\{Pt(^{N\text{-}Ph}L)_2\}_2](CF_3SO_3)_2$,[11] where $^{N\text{-}Ph}L$ is *N*-phenyl-*o*-diiminobenzosemiquinone or *N*-phenyl-*o*-diiminobenzoquinone. The three platinum complexes are assigned to ligand-based one-electron-oxidized ones of the corresponding bis-*o*-diiminobenzosemiquinone complexes. The N–C and C–C distances of $[\mathbf{2}_2]Cl_2\cdot 6H_2O$ are in good agreement with the corresponding ones of them.[11,14,15] These structural results show that the complex, $[\mathbf{2}_2]Cl_2$, is the ligand-based one-electron-oxidized complex of **2**, and that the oxidation state of the two ligands of the monomer unit in the dimer adopts a delocalized mixed-valence state belonging to class III in the classification of mixed-valence compounds of Robin and Day.[16] In other words, an unpaired electron generated by the oxidation is delocalized over two ligands of the monomer unit. Two unpaired electrons in the dimer, however, are not completely coupled with each other because $[\mathbf{2}_2]Cl_2\cdot 6H_2O$ displays a weak ESR spectrum in the solid state in our preliminary measurement. This result suggests the possibility that [**2**]I can be a dimer, though Holm et al.[4] have reported that [**2**]I is ESR active in both a solution and the solid state.

The unsupported platinum(II) complex dimers in $[\mathbf{2}_2]Cl_2\cdot 6H_2O$ form a slipped-stack columnar structure along the *c* axis with an interdimer Pt···Pt distance of 4.2063(4) Å. The crystal packing is stabilized by hydrogen bonds from the N atoms of the imino group to the Cl^- ions and to the O atoms of water molecules of crystallization (N(1)···Cl(1), N(2)···O(1), N(3)···O(2), N(4)···O(3)), from the O atoms to the Cl^- ions (O(1)···Cl(1), O(2)···Cl(1), O(3)···Cl(1)), and between the water molecules of crystallization (O(1)···O(2) and O(3)···O(1)).

Conclusion

The aqueous solution of $[Pt(H_2L)_2]Cl_2\cdot 2H_2O$ (H_2L = *o*-phenylenediamine) exhibits pH-dependent color-change behavior; the present complex changes from colorless to purple in the basic side of pH 4.5–4.6 and to yellow-green in the acidic side. In the former case, the neutral complex $[Pt(L)_2]$ is produced by the deprotonation and oxidation of the parent complex and, in the latter case, the unusual unsupported dimer complex $[\{Pt(L)_2\}_2]Cl_2\cdot 6H_2O$ is formed, where L is *o*-semibenzoquinonediimine or *o*-benzoquinonediimine. From the results, we have found that the one-electron redox process of $[Pt(L)_2]^+/[Pt(L)_2]$ is reversibly controlled by the pH of the solution. This behavior is a kind of pH-dependent chromism because of their colors being remarkably different. The phenomena is caused by the rest potential of the $[Pt(L)_2]$ solution increasing to the oxidation side across the redox potential of $[Pt(L)_2]^+/[Pt(L)_2]$ with decreasing pH to the acidic side in spite of the redox potential being invariable over the range of pH 4.0–8.0.

This work was partly supported by a Grant-in-Aid for Scientific Research (A) Project No. 12354008 from Japan Society for the Promotion of Science.

Supporting Information

Figure S1 in PDF format. This material is available free of charge on the web at: http://www.csj.jp/journals/bcsj/.

References

1 a) C. G. Pierpont, R. M. Buchanan, *Coord. Chem. Rev.* **1981**, *38*, 45. b) C. G. Pierpont, C. W. Lange, *Prog. Inorg. Chem.* **1994**, *41*, 331. c) C. G. Pierpont, *Coord. Chem. Rev.* **2001**, *216–217*, 99.

2 a) G. N. Schrauzer, *Acc. Chem. Res.* **1969**, *2*, 72. b) P. I. Clemenson, *Coord. Chem. Rev.* **1990**, *106*, 171. c) P. Cassoux, L. Valade, H. Kobayashi, A. Kobayashi, R. A. Clark, A. E. Underhill, *Coord. Chem. Rev.* **1991**, *110*, 115.

3 A. Mederos, S. Domínguez, R. Hernández-Molina, J. Sanchiz, F. Brito, *Coord. Chem. Rev.* **1999**, *193–195*, 913.

4 A. L. Balch, R. H. Holm, *J. Am. Chem. Soc.* **1966**, *88*, 5201.

5 a) R. C. Elder, D. Koran, H. B. Mark, Jr., *Inorg. Chem.* **1974**, *13*, 1644. b) H.-Y. Cheng, S.-M. Peng, *Inorg. Chim. Acta* **1990**, *23*, 169. c) J. Jubb, L. F. Larkworthy, L. F. Oliver, D. C. Povey, G. W. Smith, *J. Chem. Soc., Dalton Trans.* **1991**, 2045. d) C. Redshaw, G. Wilkinson, B. Hussain-Bates, M. B. Hursthouse, *J. Chem. Soc., Dalton Trans.* **1992**, 1803. e) B. Narayanan, M. M. Bhadbhade, *Acta Crystallogr., Sect. C* **1996**, *52*, 3049. f) K. R. Maxcy, R. Smith, R. D. Willett, A. Vij, *Acta Crystallogr., Sect. C* **2000**, *56*, e454.

6 K. Sharma, N. Fahmi, R. V. Singh, *Appl. Organomet. Chem.* **2001**, *15*, 221.

7 W. E. Cooley, D. H. Busch, *Inorg. Synth.* **1957**, *5*, 208.

8 G. M. Sheldrick, *SHELXS97* and *SHELXL97, Programs for Crystal Structure Analysis*, University of Göttingen, Germany, **1997**.

9 T. Higashi, *ABSCOR, Empirical Absorption Correction Based on Fourier Series Approximation*, Rigaku Corporation, Tokyo, Japan, **1995**.

10 L. J. Farrugia, *J. Appl. Crystallogr.* **1997**, *30*, 565.

11 D. Herebian, E. Bothe, F. Neese, T. Weyhermüller, K. Wieghardt, *J. Am. Chem. Soc.* **2003**, *125*, 9116.

12 S. Sato, M. Haruki, S. Kurita, *Acta Crystallogr., Sect. C* **1990**, *46*, 1107.

13 B. Viossat, P. Toffoli, P. Khodadad, N. Rodier, *Acta Crystallogr., Sect. C* **1987**, *43*, 855.

14 A. A. Sidorov, M. O. Ponina, S. E. Nefedov, I. L. Eremenko, Y. A. Ustynyuk, Y. M. Luzikov, *Zh. Neorg. Khim.* **1997**, *42*, 952; Translated to English: *Russ. J. Inorg. Chem.* **1997**, *42*, 853.

15 I. L. Eremenko, S. E. Nefedov, A. A. Sidorov, M. O. Ponina, P. V. Danilov, T. A. Stromnova, I. P. Stolarov, S. B. Katser, S. T. Orlova, M. N. Vargaftik, I. I. Moiseev, Y. A. Ustynyuk, *J. Organomet. Chem.* **1998**, *551*, 171.

16 M. B. Robin, P. Day, *Adv. Inorg. Chem. Radiochem.* **1967**, *10*, 247.